COMBINING TIME-DOMAIN BACK-PROJECTION AND CAPON BEAMFORMING FOR TOMOGRAPHIC SAR PROCESSING

Othmar Frey and Erich Meier

Remote Sensing Laboratories
University of Zurich, Switzerland

ABSTRACT

Various tomographic processing methods have been investigated in recent years. The quality of the focused tomographic image is usually limited by several factors. In particular, Fourier-based focusing methods are susceptible to irregular and sparse sampling, two problems that are unavoidable in case of multi-pass, multi-baseline SAR data acquired by an airborne system. Neither time-domain back-projection (TDBP) processing, although providing a very accurate processing framework, is able to overcome the problem of ambiguous target detection in the tomographic image. In this paper, a possible extension of the TDBP approach to multi-looking based tomographic focusing methods like standard beamforming and Capon beamforming is discussed. Preliminary results obtained with a simulated and a real airborne tomographic P-band data set are shown.

1. INTRODUCTION

In a single synthetic aperture radar (SAR) image multiple back-scattering elements distributed along the elevation component are projected to the two-dimensional slant-range plane and can therefore not be resolved. Pol-InSAR techniques already provide a means to discriminate a limited number of scattering elements in the elevation direction from a single-baseline dataset. By tomographic processing of multi-baseline SAR data, however, it is possible to resolve the ambiguity in the elevation component and therefore this technique is suitable to produce true three-dimensional images. Hence, different back-scattering elements within a volume can directly be localized. This property can be exploited for the reconstruction of volumetric structures as forested areas, as well as for a more detailed imaging of built-up areas and mountainous regions, which exhibit a high percentage of layover regions. The most common approach, the Fourier based SPECAN (SPECtral ANalysis) technique, which has been adopted in [1], requires that the synthetic aperture is sampled regularly and densely. This requirement is not met in case of airborne SAR data of multiple acquisition paths, and the synthetic aperture in the normal direction is sampled sparsely. As a result, the tomographic image is subject to defocusing,
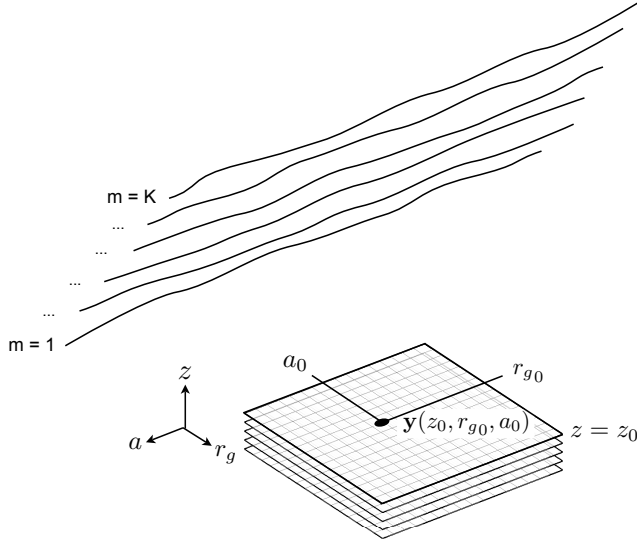
high side lobes and ambiguities in the normal direction. In order to overcome the ambiguity problem and to improve the resolution modern spectral estimation methods have been proposed as a substitute to spectral estimation by FFT. These methods include spectral estimation by the Capon method [2] and subspace-based spectral estimators such as the MUSIC algorithm [3, 4]. These methods replace the last step, the spectral estimation by FFT, but geometric approximations made in a previous processing step are still present in the data.

Recently, we have investigated a different approach, namely to process airborne multi-baseline data completely in the time domain in order to be able to account for the complex, non-uniform acquisition geometry. The approach has been applied to an airborne multi-baseline data set and first results were presented in [5]. Despite of having achieved a good focusing performance in terms of resolution, the suppression of anomalous side lobes and ambiguous targets is still a problem.

In this paper, we discuss a modified time-domain tomographic processing approach, namely a combination of standard TDBP processing for azimuth focusing and time-domain multi-looking based focusing methods for tomographic focusing in the normal direction. A common formulation is given for the three approaches which are known as the TDBP algorithm, the standard beamforming and the Capon beamforming algorithm. Standard TDBP/beamforming and the Capon beamformer are both non-parametric methods for direction of arrival estimation, i.e., they make no assumption about the covariance structure of the data [6]. The tomographic data is to be focused to a three-dimensional reconstruction grid as detailed in [5] thereby omitting critical resampling and coregistration steps that are required by Fourier-based methods.

2. DATA MODEL AND ACQUISITION GEOMETRY

In Fig. 1 a tomographic flight pattern is depicted representing the airborne case where motion deviations from ideally linear and parallel flight tracks are present. In addition, the three-dimensional reconstruction grid to which the data are focused within our time-domain processing scheme is depicted. There

$$\mathbf{y}(z_0, r_{g_0}, a_0) = [y_1(z_0, r_{g_0}, a_0) \ \dots \ y_K(z_0, r_{g_0}, a_0)]^T$$

Fig. 1. Tomographic acquisition pattern and the three-dimensional reconstruction grid. $\mathbf{y}(z_0, r_{g_0}, a_0)$ is a vector containing the azimuth focused signals from K flight tracks at position (z_0, r_{g_0}, a_0) of the reconstruction grid. r_g is the ground range, a is the azimuth direction, and z indicates the height within the imaged volume.

are K individual flight tracks flown in a ideally parallel fashion. The vector $\mathbf{y}(z_0, r_{g_0}, a_0)$ contains the azimuth focused signals from K flight tracks at position (z_0, r_{g_0}, a_0) of the reconstruction grid. In general, the signal vector $\mathbf{y}$ is:

$$\mathbf{y}(z, r_g, a) = [y_1(z, r_g, a) \ \dots \ y_K(z, r_g, a)]^T \qquad (1)$$

where r_g is the ground range position, a is the azimuth position, and z indicates the height within the imaged volume.

For the sake of readability, the horizontal positioning (r_g and a) of the data vector is omitted in the following. Hence, $\mathbf{y}(z)$ is the signal for a specific voxel at height z.

3. STANDARD TDBP AS A SPECIAL CASE OF MULTI-LOOK BEAMFORMING

The TDBP tomographic focusing scheme presented in [5] can be written as follows:

$$v(z) = \sum_{m=1}^{K} y_m(z) \cdot e^{i2k_c(r_m(z) - r_1(z))}, \qquad (2)$$

where $v(z)$ is the focused signal at height z (for a specific ground-range/azimuth position), K is the number of flight tracks that build the tomographic pattern, $y_m(z)$ is the azimuth-focused signal from flight track m for that specific ground-range/azimuth pixel focused to a reconstruction grid at height z. k_c is the central wavenumber and $r_m(z)$ is the closest range distance between the source at height z and the m-th flight track. There are two modifications in the notation of eq. (2) compared with the formulation in [5]. The first modification is that the focused data are demodulated with respect to a master track $m = 1$ and, the second, that the range distance multiplication is assumed to be included in the term $y_m(z)$.

Using the following two vector notations, a steering vector $\mathbf{a}(z)$:

$$\mathbf{a}(z) = [1 \ e^{i\varphi_2(z)} \ \dots \ e^{i\varphi_K(z)}]^T, \qquad (3)$$

with $\varphi_m(z) = -2k_c(r_m(z) - r_1(z))$, $m = 1, .., K$; and a signal vector $\mathbf{y}(z)$:

$$\mathbf{y}(z) = [y_1(z) \ \dots \ y_K(z)]^T, \qquad (4)$$

the focused signal $v(z)$ of eq. (2) can be written as:

$$v(z) = \mathbf{a}^H(z)\mathbf{y}(z). \qquad (5)$$

Then, the power image $\hat{P}_T(z) = |v(z)|^2$, i.e., the focused signal obtained from TDBP processing for a certain ground-range azimuth position on a horizontal layer at height z is:

$$\begin{align}
\hat{P}_T(z) &= |v(z)|^2 = |\mathbf{a}^H(z)\mathbf{y}(z)|^2 \qquad (6) \\
&= \mathbf{a}^H(z)\mathbf{y}(z)\mathbf{y}(z)^H\mathbf{a}(z) \qquad (7) \\
&= \mathbf{a}^H(z)\left(\hat{\mathbf{R}}_y(z)\right)_{N=1}\mathbf{a}(z). \qquad (8)
\end{align}$$

$\mathbf{y}(z)\mathbf{y}(z)^H$ corresponds to the sample covariance matrix $\hat{\mathbf{R}}_y(z)$ of the standard beamformer [6] in the case where the number of looks $N = 1$:

$$\hat{\mathbf{R}}_y(z) = \frac{1}{N} \sum_{n=1}^{N} \mathbf{y}(n, z)\mathbf{y}^H(n, z) \qquad (9)$$

In other words, the power image after time-domain back-projection processing can be interpreted as the standard beamforming method for the single-look case $N = 1$.

Compared to the usual formulation of beamforming [6, 2] there is one substantial difference with respect to how the focusing in normal direction is carried out: In our TDBP-based processing scheme a new covariance matrix $\hat{\mathbf{R}}_y(z)$ is calculated for each horizontal layer (distinguished by the height z) of the reconstruction grid. Recall, that within our approach, the SAR data from the K different flight tracks are focused and thereby coregistered directly on a three dimensional reconstruction grid. So, given a back-scatterer located at height $z = z_0$ and non-linear airborne flight tracks, a target will be reconstructed best for all K flight tracks – in terms of azimuth focusing – when it is focused on the horizontal layer at the correct height $z = z_0$. And as a consequence, the azimuth-focused signals from the K flight tracks should be more similar at a particular ground-range azimuth coordinate at the correct height $z = z_0$ than for all other heights $z \neq z_0$. This
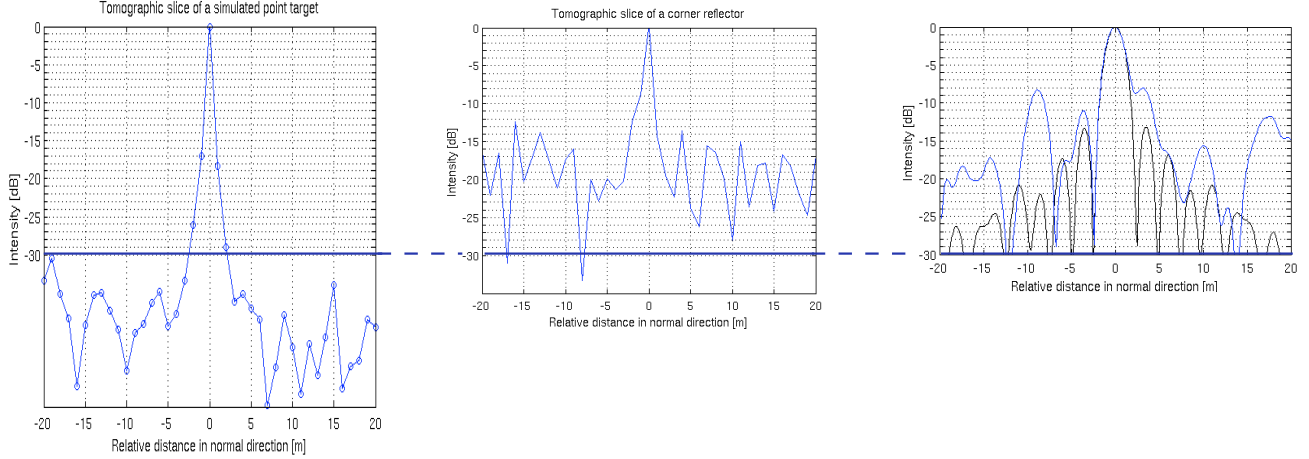
Fig. 2. Left: Multi-look Capon beamforming of a simulated point target. Center: Multi-look Capon beamforming of an in-scene corner reflector. Right: TDBP 3D focusing of a simulated point target (black line) and the in-scene corner reflector (blue line).

is the motivation to calculate the sample covariance matrix $\hat{\mathbf{R}}_y(z)$ separately for each height z and this is also, besides the different azimuth focusing technique, the difference to the Capon beamforming approach proposed by Lombardini et al. [2].

3.1. Multi-Look Standard Beamforming

There are several possibilities in terms of improving the focusing quality and the sidelobe level of the tomographic image while maintaining the time-domain focusing scheme to a 3D reconstruction grid.

A proximate step towards a better estimation of the tomographic signal is processing the data to N looks, which are assumed to be independent and identically distributed. However, multi-looking is at the expense of the resolution in ground range and azimuth. Processing multiple looks in the time-domain corresponds to the standard beamforming approach where the sample covariance matrices, which are calculated for each look, are averaged as in eq. (9):

$$\hat{P}_B(z) = \mathbf{a}^H(z)\hat{\mathbf{R}}_y(z)\mathbf{a}(z) \tag{10}$$

3.2. Multi-Look Capon Beamforming

In a similar way Capon beamforming can be applied within our time-domain 3D focusing framework. After matrix inversion of the sample covariance matrix $\hat{\mathbf{R}}_y(z)$ the Capon estimated power $\hat{P}_C$ is obtained for each layer on height z:

$$\hat{P}_C(z) = \frac{1}{\mathbf{a}^H(z)\hat{\mathbf{R}}_y(z)^{-1}\mathbf{a}(z)} \tag{11}$$

Lombardini et al. [2] have proposed to include diagonal loading when building the sample covariance estimate $\hat{\mathbf{R}}_\mathbf{y}(\mathbf{z})$

because of the non-uniform alignment of the phase centers which build the synthetic aperture in the normal direction.

4. PROCESSING APPROACHES

As proposed in [5] for TDBP focusing in azimuth and for tomographic focusing, the multi-baseline data are again processed directly to a three-dimensional reconstruction grid. But, since for multi-look standard beamforming and Capon beamforming the sample covariance matrix $\hat{\mathbf{R}}_\mathbf{y}(\mathbf{z})$ has actually to be calculated the data are demodulated after the TDBP azimuth focusing to the various layers. We also have to keep track of the range distances at the closest point of approach used for demodulation. They are needed to build the appropriate steering vectors.

Lombardini et al. [2] apply Capon beamforming for tomographic focusing after having processed the data by the extended chirp scaling algorithm and after having coregistered the focused data sets from the K flight tracks to a common geometry. They calculate *one* sample covariance matrix $\hat{\mathbf{R}}_\mathbf{y}$ for a certain pixel in this coregistered range-azimuth geometry, therefore, $\hat{\mathbf{R}}_\mathbf{y}$ does not depend on the height z. In contrast, we process and thereby coregister the data directly onto several (horizontal) layers and, in particular, we also calculate a sample covariance matrix $\hat{\mathbf{R}}_\mathbf{y}(z)$ *for each layer* on height z. So, a data vector $\mathbf{y}_z(n,z)$ is set up for each height z and for each look. $\hat{\mathbf{R}}_\mathbf{y}(z)$ is then calculated from the demodulated K data sets on a particular height z. The high geometric fidelity that is maintained by following this time-domain approach has the potential to lead to an improved focusing quality of the tomographic images.

5. PRELIMINARY RESULTS

In Fig. 2 tomographic slices in normal direction for simulated and real point targets corresponding to an airborne P-band data set are depicted — for a description of the airborne tomographic P-band data set the reader is referred to [5]. The plot on the left-hand side of Fig. 2 shows the tomographic image of a simulated point target after multi-look Capon beamforming, and the central plot shows the impulse response of an in-scene corner reflector obtained by tomographic focusing of the real P-band data set; again using multi-look Capon beamforming. On the right-hand side, the tomographic images of a simulated point target (black line) and the in-scene corner reflector (blue line) are given as they result from standard 3D TDBP processing.

6. DISCUSSION AND SUMMARY

Pure TDBP-based tomographic focusing and a modification thereof in the form of a multi-look (Capon) beamformer for the focusing step in the normal direction has been presented and discussed.

Preliminary results obtained with these processing methods have been shown by means of an airborne P-band data set and corresponding simulated data, respectively.

A known problem [5] with the pure 3D TDBP algorithm is that high intensity values are accompanied by considerable sidelobes and ambiguities in the normal direction

The proposed combination of TDBP and multi-look Capon beamforming yields an enhanced suppression of the sidelobes for the simulated point target compared to the pure 3D TDBP focusing method. However, the focusing performance obtained with the in-scene corner reflector is inferior to the simulated case, so far. This is most likely due to remaining calibration errors in the steering vectors and due the critical matrix inversion step, where diagonal loading is required.

Further steps include the investigation of methods in order to stabilize the Capon beamformer, and, after the calibration issue is solved, a larger subset of the tomographic P-band data set of a forested area will be evaluated using this technique.

7. ACKNOWLEDGMENT

8. REFERENCES

[1] A. Reigber and A. Moreira, "First Demonstration of Airborne SAR Tomography Using Multibaseline L-Band Data," *IEEE Transactions on Geoscience and Remote Sensing*, vol. 38, no. 5, pp. 2142–2152, 2000.

[2] F. Lombardini and A. Reigber, "Adaptive spectral estimation for multibaseline SAR tomography with airborne L-band data," in *IEEE International Geoscience and Remote Sensing Symposium, IGARSS'03.*, vol. 3, 2003, pp. 2014–2016.

[3] S. Guillaso and A. Reigber, "Polarimetric SAR Tomography (POLTOMSAR)," in *Proceedings of POLINSAR'05*, Frascati, Italy, 2005.

[4] F. Gini and F. Lombardini, "Multibaseline Cross-Track SAR Interferometry: A Signal Processing Perspective," *IEEE Aerospace and Electronic Systems Magazine*, vol. 20, no. 8, pp. 71–93, 2005.

[5] O. Frey, F. Morsdorf, and E. Meier, "Tomographic Processing of Multi-Baseline P-Band SAR Data for Imaging of a Forested Area," in *IEEE International Geoscience and Remote Sensing Symposium, IGARSS'07*, 2007.

[6] P. Stoica and R. L. Moses, *Spectral Analysis of Signals*. Prentice Hall, 2005.